Electrochemical and Solid-State Letters, **13** (7) K67-K71 (2010)
1099-0062/2010/13(7)/K67/5/$28.00 © The Electrochemical Society

Fabrication and Characteristics of β-Bi_2O_3 Nanowires Prepared by Heating a Mixture of In and Bi Powders

Hyoun Woo Kim,[a,z] Han Gil Na,[a] Ju Chan Yang,[a] Hyo Sung Kim,[a] Ji-Hye Lee,[b] and Keon-Ho Yoo[b]

[a]*Division of Materials Science and Engineering, Inha University, Incheon 402-751, Republic of Korea*
[b]*Department of Physics, Kyung Hee University, Seoul 130-701, Republic of Korea*

We studied the characteristics of tetragonal β-Bi_2O_3 nanowires synthesized by heating a mixture of Bi and In powders. Sufficient growth time and In powder ratio are required for the generation of nanowires. Based on our observations, we propose a Au-catalyzed vapor–liquid–solid process as the dominant growth mechanism, in which In powder affects the morphology of nanowires. Photoluminescence (PL) analysis indicates that the nanowires exhibit emission bands centered at 1.58, 2.40, and 2.76 eV, regardless of the measurement temperature. The overall PL intensity tends to decrease as the measurement temperature increases.
 [DOI: 10.1149/1.3387710]

Manuscript submitted December 29, 2009; revised manuscript received March 17, 2010. Published April 15, 2010.

Bismuth oxide (Bi_2O_3), which is a very important dielectric material, has attracted great attention due to its various applications, including optical coatings, microelectronics, ceramic glass manufacturing, solar cells, and gas sensors. One-dimensional (1D) nanomaterials have extraordinary physical and chemical properties compared to bulk materials, with their finite size confining the electron wave functions, which results in quantized energy levels and a significant modification of the transport and optical properties. Accordingly, a study on the Bi_2O_3 1D nanomaterials is urgently needed.

In spite of their importance, only a few studies have been published on the fabrication of Bi_2O_3 1D nanomaterials, and in those studies researchers have used atomic-pressure chemical vapor deposition (CVD)[1] and metallorganic CVD.[2] The slow oxidation of Bi nanowires up to 500°C resulted in the fabrication of Bi–Bi_2O_3 core-shell nanowires, with the subsequent fast oxidation up to 750°C converting the Bi–Bi_2O_3 core-shell nanowires to single-crystalline Bi_2O_3 nanotubes.[3] However, before the present study, the lowest temperature synthetic route reported for the growth of Bi_2O_3 nanowires with a compact and single-phased structure was 800°C, which was achieved by using oxidative metal vapor-phase deposition.[4] In the present article, we fabricated Bi_2O_3 nanowires at a temperature of 500°C via a simple heating process. This method can provide a low cost, simple, and low temperature process, which could pave the way for the application of Bi_2O_3 nanowires in future ultralarge-scale integration devices. In addition to this process, we suggest a growth mechanism for Bi_2O_3 nanowires. The role of In as well as Au is discussed. We also studied the photoluminescence (PL) spectra of Bi_2O_3 nanowires in terms of their dependence on measurement temperature. Among the various polymorphs of Bi_2O_3 (such as α-, β-, γ-, δ-, and ω-Bi_2O_3), β-Bi_2O_3 is a metastable phase, which exhibits a promising ionic conductivity from deliberate doping.[5,6] In addition, β-Bi_2O_3 generates atomic oxygen under certain conditions. This oxygen transforms into ozone in the gas phase.[7] β-Bi_2O_3 is thus an efficient oxygen donor and is a promising catalyst. β-Bi_2O_3 has a smaller bandgap of 2.58 eV at 300 K, which is significantly smaller than that of α-Bi_2O_3 (2.85 eV), exhibiting distinct optical and photoelectrical properties.[8] In the present study, we synthesized β-Bi_2O_3 nanowires.

Experimental

The Bi_2O_3 nanowires reported here were synthesized in a quartz tube by directly heating a mixture of Bi and In powders. In a carrier gas of Ar and dioxide (O_2) with a constant total pressure of 1 Torr, the percentage of O_2 partial pressure was set at about 3%. The reaction temperature was set at 500°C and the growth was conducted for 1–3 h. With the total weight of the powder mixture being kept at 2 g, the In power ratio was set to 0, 0.25, and 0.5. Herein, the In powder ratio is defined as the weight of the In powder divided by the total weight of the powder mixture (In + Bi). A Au-coated silicon (Si) (100) substrate (about 3 nm) was used to collect the product.

The as-collected product was examined by an X-ray diffractometer (XRD; Philips X'pert MRD diffractometer), scanning electron microscope (SEM, Hitachi S-4300 SE), and transmission electron microscopy (TEM). The PL measurements of the samples were carried out using a 325 nm line from a He–Cd laser (KIMMON, ik3102 R-G) as an excitation source. The sample temperature was set at 18, 100, 200, and 300 K using a He closed cycle refrigerator (JANIS CCS-100). The signal was detected with a cooled photomultiplier tube (ISA Jobin Yvon R955) through a lock-in amplifier (Princeton Applied Research 5210).

Results and Discussion

Figure 1a-c shows top-view SEM images of the samples for the growth times of 1, 2, and 3 h, respectively, in which the In powder ratio was maintained at 0.5. It is observed that the amount of 1D nanostructures increased as growth time increased. The upper right insets in Fig. 1b and c indicate that the nanostructures have a 1D morphology, with a nanoparticle at the tip.

To investigate the role of In, we varied the ratio of the In powder in a powder mixture with a fixed total weight of 2 g. While Fig. 1c shows the SEM image of the product with 1 g of In powder, Fig. 1d shows a top-view SEM image of the product with 0.5 g of In powder, which exhibits some clusterlike structures without growing nanowires. Figure 1e shows a top-view SEM image of the product without In powder. The product has filmlike structures, with some large clusterlike structures. Sufficient addition of In powder is required for the growth of 1D nanostructures. Figure 2 shows an XRD pattern of the sample shown in Fig. 1c. Apart from the Au-related peaks from the Au catalyst, all recognizable diffraction peaks can be indexed to the tetragonal β-Bi_2O_3 with the lattice constants a = 7.741 Å and c = 5.634 Å (JCPDS 78-1793).

A low magnification TEM image of a nanowire is shown in Fig. 3a, indicating that the nanowire in the form of a solid rod has a dark nanoparticle at the tip. The diameter of the nanoparticle is estimated to be 30–40 nm. Energy-dispersive X-ray (EDX) measurements made on the wire tip and the wire stem indicate that the nanowire tip is composed of Au elements, whereas the nanowire stem is only composed of Bi and O (Fig. 3b and c). Ni and C signals are generated from the Ni grid coated with a porous carbon film, supporting the nanowires. Figure 3d shows an associated selected area electron diffraction (SAED) pattern exhibiting diffraction rings of β-Bi_2O_3. Although they appear to be diffraction spots, close examination reveals that they are rings, rather than spots. Figure 3e shows a representative high resolution transmission electron microscopy (HRTEM) image enlarging an outer region of the nanowire stem.

[z] E-mail: hwkim@inha.ac.kr

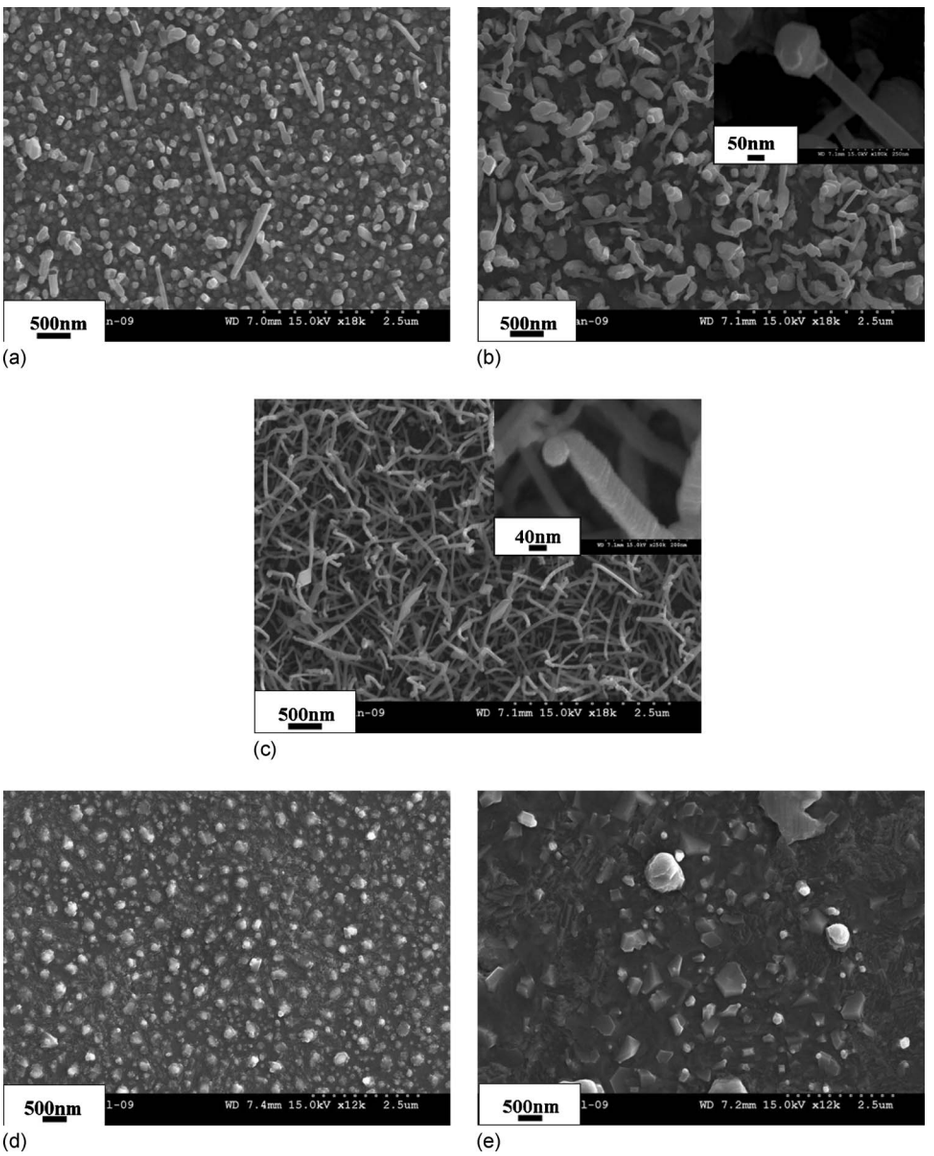

Figure 1. Top-view SEM images of the samples for growth times and In powder ratios of (a) 1 h and 0.5, (b) 2 h and 0.5, (c) 3 h and 0.5, (d) 3 h and 0.25, and (e) 3 h and 0, respectively. The upper right insets correspond to the enlarged images of typical nanowires.

The spacings between the lattice planes are about 0.31 and 0.34 nm, corresponding to the spacings d_{201} and d_{210} of the tetragonal β-Bi_2O_3.

Owing to the presence of Au catalyst particles, which were observed at the ends of the 1D structures from the SEM and TEM analyses, the growth in the present study corresponds to the vapor–liquid–solid (VLS) process. Herein, during the evaporation process, Bi powder can be evaporated to become Bi vapor, eventually combining with a Au film on the substrate surface. The addition of Bi lowers the melting point of Au, presumably forming a liquid phase. Subsequently, the solid Bi_2O_3 starts to grow on the liquid-phase surface, eventually forming the Bi_2O_3 nanowires. Although it is evident that Au played a catalytic role in synthesizing the Bi_2O_3 nanowires, the role of In remains unclear.

Our previous experiments revealed that a high temperature process (~700°C) was required to obtain Bi_2O_3 nanowires when In powder was not used. Accordingly, the low melting point of In (157°C) provided a new opportunity to lower the growth temperature of the Bi_2O_3 nanowires in the VLS process, which would be favorable for device integration. In Fig. 1c-e, we demonstrate that the addition of In powder facilitated the growth of 1D structures. No In or In-associated compounds formed in the products, according to

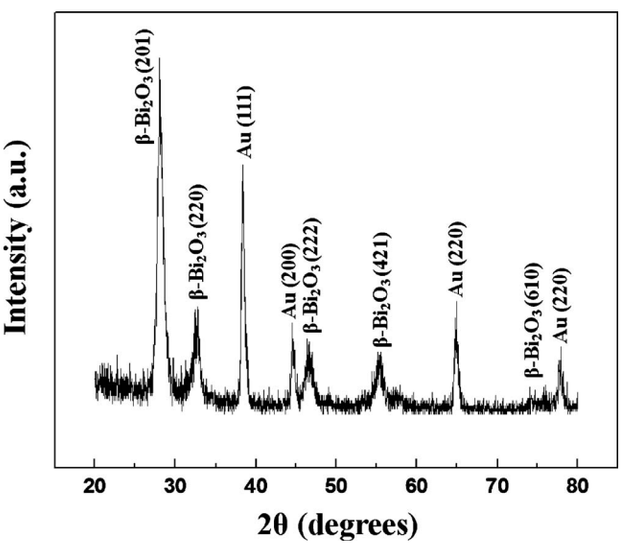

Figure 2. XRD pattern of Bi_2O_3 nanowires.

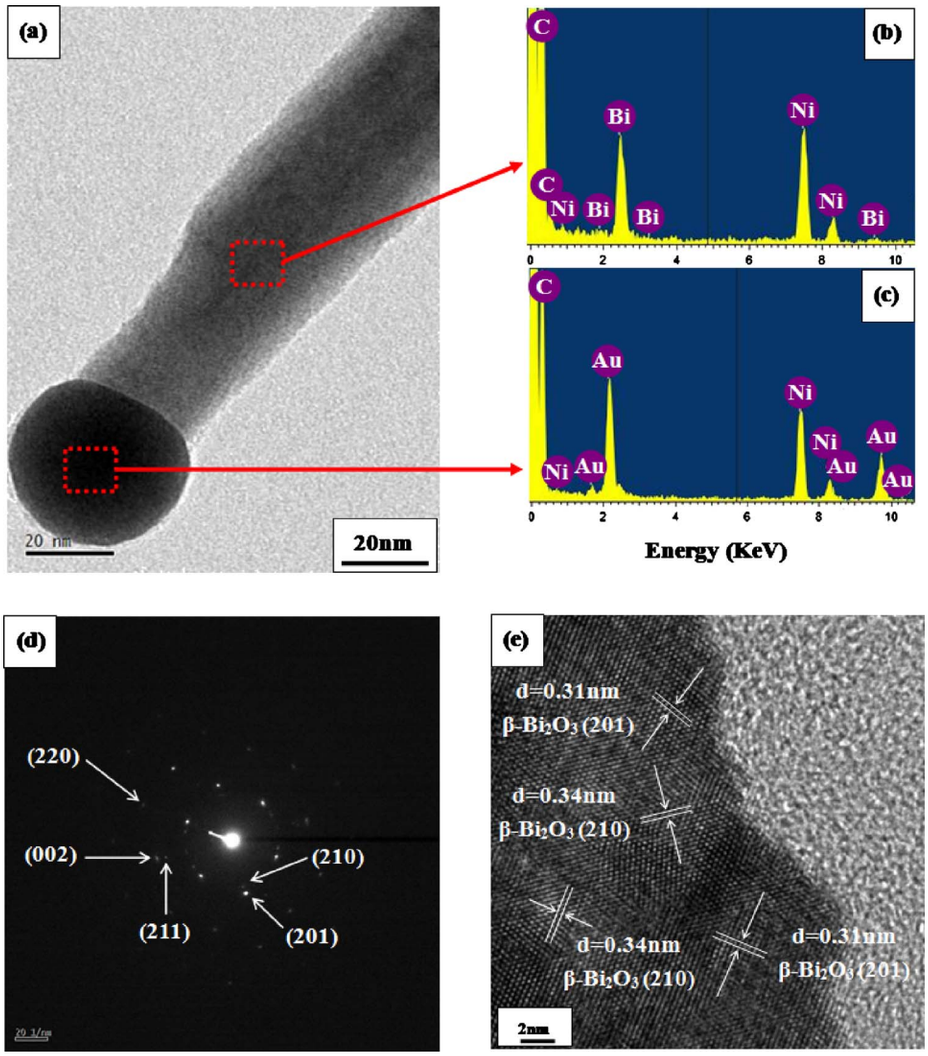

Figure 3. (Color online) (a) TEM image of a Bi_2O_3 nanowire. EDX spectra taken from the (b) stem and (c) tip part of Bi_2O_3 nanowire. The C and Ni shown in the spectrum originate from the TEM C-coated Ni grid. (d) Corresponding SAED pattern. (e) HRTEM image from the stem region of a Bi_2O_3 nanowire.

the XRD analysis (Fig. 2). Also, In concentration in the nanowire and catalyst particle was below the detection limit of the TEM-EDX analysis (Fig. 3b and c).

Based on the above observations, we have speculated on the growth mechanism of the nanowires. One possibility is that In vapor is adsorbed onto Au, forming a complex Au–Bi–In–O fluid phase (in this case, ambient O_2 is also adsorbed onto the liquid droplet). This is certified by the Au–In and Bi–In binary phase diagram, indicating that the melting point should decrease as a result of the addition of In.[9] The addition of In may induce less supercooling and, thus, secondary growth from the stem rods is suppressed. Instead, relatively thin 1D structures are favored. With the growth of Bi_2O_3 nanowires, the Au–In liquid droplet eventually solidifies and the Au nanoparticles form with the In species segregated on the nanoparticle surface and subsequently removed. Another possibility is that In vapor can reduce Au diffusion along the sidewall of the nanowire away from the catalyst droplets, permitting the droplet volume to remain constant for a longer period of time. A similar phenomenon was observed in Si nanowires, in which oxygen vapor played a role in maintaining the liquid droplet.[10] Furthermore, In may enhance the adatom mobility on the nanowire surface,[11] facilitating the incorporation of Bi and O species into the liquid droplet and thus the further growth of Bi_2O_3 nanowires. More research is needed to define the detailed role of In in the present growth process.

Figure 4a shows the PL emission spectra of the products measured at 18, 100, 200, and 300 K. The broad emission spectra can be divided into three Gaussian functions, which were centered at 2.76, 2.40, and 1.58 eV, respectively. The peak positions of the 2.76, 2.40, and 1.58 eV centered emissions exhibited no noticeable shift with the change in the measurement temperature in the range of 18–300 K. For example, the fitting procedure for 18 and 300 K PL spectra using Gaussian components is shown in Fig. 4b and c, respectively. For 2.76 eV centered bands, a similar blue emission was observed from Bi_2O_3 nanorods produced via the metallorganic CVD,[2] and Bi_2O_3 nanoparticles were synthesized via a microemulsion method.[12] For the 2.40 eV centered band, a similar green emission shoulder peak was observed from the PL spectrum of bismuth oxide nanostructures.[13]

The luminescence bands at the energy of 2.4–3.1 eV were reported in Bi_2O_3-based oxide glass systems.[14] In particular, it is possible that the visible (blue[13] or green[13,15]) emission band arises from Bi^{3+} ions,[13,15] based on the mechanism, including internal transitions of Bi^{3+} ions, in which an intraionic transition of Bi^{3+} ($^3P_0 \rightarrow {}^1S_0$) is considered to be the origin of the luminescence bands.[16] Also, the blue emission band may originate from defects in the crystal and can be attributed to the recombination of the conduction band with the energy levels of deep-trap or surface state.[12] For 1.58 eV centered bands, a similarly broadened emission and the emission maxima between 1.6 and 1.9 eV were observed in the PL spectra of 1D Bi_2O_3 nanohooks.[17] Such low energy emission is attributed to the crystal defects or defect levels associated with the defects, in-

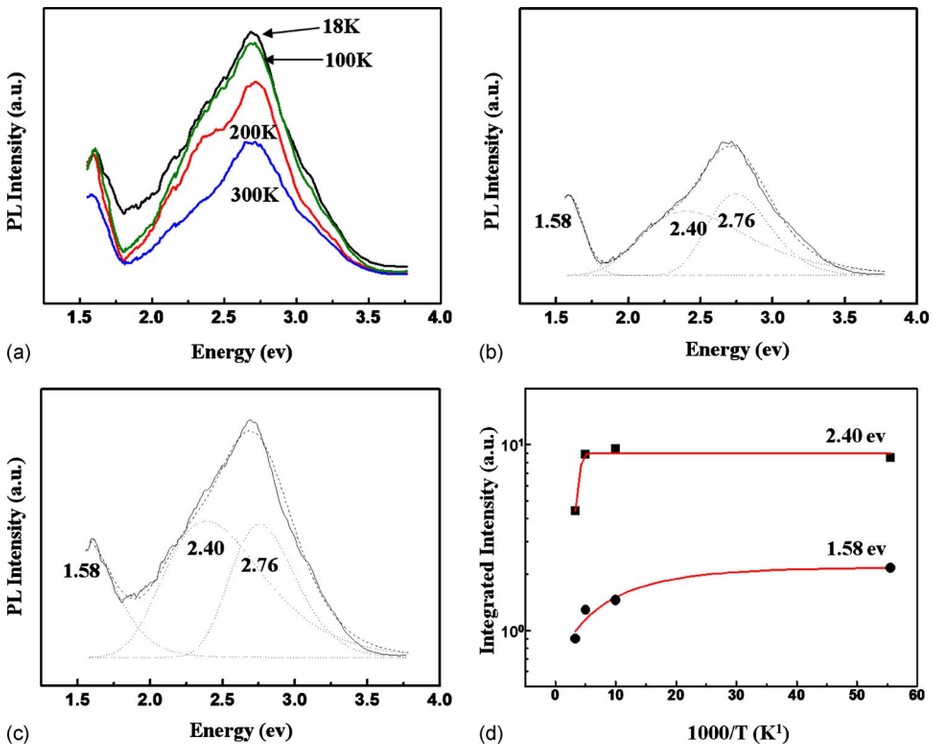

Figure 4. (Color online) (a) PL spectra excited by 325 nm light for the samples at 18, 100, 200, and 300 K. Gaussian deconvolution of the PL spectra measured at (b) 300 and (c) 18 K. (d) Temperature dependence of the integrated PL intensity for 2.40 and 1.58 eV centered emissions.

cluding oxygen vacancies that formed during growth. A considerable amount of vacancy-related defects can be generated during the synthesis of Bi_2O_3 nanowires.[17] It is possible that emissions around ~1.5 to 1.8 eV are related the Bi^{3+}-intraionic transition of $^3P_0 \rightarrow {}^1D_2$ and $^3P_0 \rightarrow {}^3P_2$, respectively.[9]

The overall PL intensity tends to decrease as the measurement temperature increased (Fig. 4a), as seen in previous articles.[18] The integrated PL intensities of the 2.40 and 1.58 eV centered emissions are plotted in Fig. 4d as a function of temperature. Being analogous to previous PL data from other materials, including CdTe,[19] $NaTaO_3$,[20] Y_2O_3:Bi,[16] ZnS:Mn^{2+},[21] InGaN/GaN,[22] and ZnMnO,[23] the experimental data from Bi_2O_3 nanowires follow an Arrhenius-type temperature dependence, which can be described by $I(T) = I_0/[1 + C\ \exp(-E_a/k_BT)]$, where C is a fitting constant,[24] I_0 is the PL intensity at 0 K, E_a is the thermal activation energy (or thermal quenching energy), and k_B is the Boltzmann constant.[20] By fitting each data set in Fig. 4d to the above equation, the thermal activation energy (E_a) of 2.40 and 1.58 eV centered emissions is estimated to be about 10.0 and 6.2 meV, respectively. These values are comparable to the values (5–19 meV) obtained from bismuth (Bi^{3+})-activated oxides.[16] Accordingly, the temperature dependence of the PL intensities of the 2.40 and 1.58 eV centered emissions can be explained by the thermal quenching theory. Reshchikov et al. proposed that the temperature dependence of the PL integrated intensity is associated with the thermal escape of holes from the defects to the valence band.[18,25] They suggested that the acceptors responsible for the visible emissions included V_{Ga} associated with a variety of defects.[18] Also, it is possible that one configuration of the defect, perhaps a charge state, is more stable at low temperature.[22] Further systematic investigation is underway to reveal the associated mechanisms of the temperature dependence of PL intensity.

Conclusion

We have successfully fabricated Bi_2O_3 nanowires by heating a mixture of Bi and In powders at 500°C. XRD and TEM investigations confirm that the nanowires were crystalline with a tetragonal β-Bi_2O_3 phase. Thin 1D structures could be generated with this process, given sufficient growth time and In powder ratio. The growth of Bi_2O_3 nanowires was controlled by a VLS mechanism. Both Au and In played a catalytic role in growing Bi_2O_3 nanowires. We discussed the mechanism by which the addition of In facilitated the growth of nanowires. Gaussian deconvolution analysis revealed that the PL spectra comprised emission bands centered at 1.58, 2.40, and 2.76 eV, regardless of the measurement temperature, in the range of 18–300 K. The overall PL intensity tends to decrease with an increase in measurement temperature. The thermal quenching energies of 2.40 and 1.58 eV centered emissions are estimated to be about 10.0 and 6.2 meV, respectively.

Acknowledgments

This research was supported by the Basic Science Research Program through the National Research Foundation of Korea (NRF) funded by the Ministry of Education, Science and Technology (2009-0073723).

Inha University assisted in meeting the publication costs of this article.

References

1. X. P. Shen, S. K. Wu, and H. Zhao, *Physica E (Amsterdam)*, **39**, 133 (2007).
2. H. W. Kim, J. W. Lee, and S. H. Shim, *Sens. Actuators B*, **126**, 306 (2007).
3. L. Li, Y.-W. Yang, G.-H. Li, and L.-D. Zhang, *Small*, **2**, 548 (2006).
4. Y. Qiu, D. Liu, and S. Yang, *Adv. Mater.*, **18**, 2604 (2006).
5. W. Zhou, D. A. Jefferson, M. Alario-Franco, and J. M. Thomas, *J. Phys. Chem.*, **91**, 512 (1987).
6. V. V. Kharton, E. N. Naumovich, A. A. Yaremchenko, and F. M. B. Marques, *J. Solid State Electrochem.*, **5**, 160 (2001).
7. O. V. Udalova, A. N. Romanov, Yu. N. Rufov, D. P. Shashkin, and A. M. Kulizade, *Kinetics and Catalysis*, **43**, 81 (2002).
8. L. Leontie, M. Caraman, M. Alexe, and C. Harnagea, *Surf. Sci.*, **507–510**, 480 (2002).
9. X.-G. Meng, J.-R. Qiu, M.-Y. Peng, D.-P. Chen, Q.-Z. Zhao, X.-W. Jiang, and C.-S. Zhu, *Opt. Express*, **13**, 1635 (2005).
10. S. Kodambaka, J. B. Hannon, R. M. Tromp, and F. M. Ross, *Nano Lett.*, **6**, 1292 (2006).
11. O. Landré, R. Songmuang, J. Renard, E. Bellet-Amalric, H. Renevier, and B. Daudin, *Appl. Phys. Lett.*, **93**, 183109 (2008).
12. W. Dong and C. Zhu, *J. Phys. Chem. Solids*, **64**, 265 (2003).
13. L. Kumari, J.-H. Lin, and Y.-R. Ma, *Nanotechnology*, **18**, 295605 (2007).
14. M. Komatsu, K. Oyoshi, S. Hishita, K. Matsuishi, S. Onari, and T. Arai, *Mater.*

Chem. Phys., **54**, 286 (1998).
15. A. M. Srivastava and W. W. Beers, *J. Lumin.*, **81**, 293 (1999).
16. O. M. Bordun, *J. Appl. Spectrosc.*, **69**, 67 (2002).
17. L. Kumari, J.-H. Lin, and Y.-R. Ma, *J. Phys.: Condens. Matter*, **19**, 406204 (2007).
18. M. A. Reshchikov and R. Y. Korotkov, *Phys. Rev. B*, **64**, 115205 (2001).
19. A. E. Saunders, B. Koo, X. Wang, C.-K. Shih, and B. A. Korgel, *ChemPhysChem*, **9**, 1158 (2008).
20. Y.-C. Lee, H. Teng, C.-C. Hu, and S.-Y. Hu, *Electrochem. Solid-State Lett.*, **11**, P1 (2008).
21. W. Chen, F. Su, G. Li, A. G. Joly, J.-O. Malm, and J.-O. Bovin, *J. Appl. Phys.*, **92**, 1950 (2002).
22. T. B. Hoang, L. V. Titova, H. E. Jackson, L. M. Smith, J. M. Yarrison-Rice, J. L. Lensch, and L. J. Lauhon, *Appl. Phys. Lett.*, **89**, 123123 (2006).
23. S. Lee, Y. Shon, and D. Y. Kim, *Thin Solid Films*, **516**, 4889 (2008).
24. J. Yu, H. Liu, Y. Wang, F. E. Fernandez, and W. Jia, *J. Lumin.*, **76–77**, 252 (1998).
25. M. A. Reshchikov and H. Morkoc, *J. Appl. Phys.*, **97**, 061301 (2005).